A method of suppressing liquefaction using a solidification material and tension stiffeners

Une méthode de prévention de la liquéfaction par cimentation et précontrainte

Nakamichi M., Sato K.
Fukuoka University

ABSTRACT: The Great Eastern Japan Earthquake occurred on March 11, 2011 and caused significant liquefaction damage. This obviously occurred in the Tohoku region, especially the Kanto region, but has also been a serious problem in the Tokyo bay coast landfilled area and inland areas. Therefore, this research focuses on popular cement solidification methods with the addition of short fibers. These are expected to increase the apparent cohesion. The effects of these additives are investigated herein. This paper reports on the results of basic research conducted and whether these techniques lead to suppression of liquefaction related to the duration of earthquakes.

RÉSUMÉ : Suite à la catastrophe du 11 mars 2011, le Japon fait face à des dégâts liés à la liquéfaction des sols d'une ampleur sans précédent. Ce phénomène est devenu un problème d'une grande gravité dans la région de Tohoku évidemment, mais également dans celle du Kantô, et notamment sur les terre-pleins de la baie de Tokyo, ainsi qu'à l'intérieur des terres. Dans cette étude, nous avons analysé l'évolution de la force d'adhésion de l'apparence des matériaux précontraints, ainsi que le processus de solidification du ciment dans les méthodes de résistances à la liquéfaction. Nous présenterons les résultats de cette étude pour comprendre comment ces méthodes peuvent être corrélées à la résistance à la liquéfaction, contre les mouvements sismiques.

KEYWORDS: suppression of liquefaction, cohesion, frequency

1 INTRODUCTION

Japan is one of the most earthquake prone countries in the world. Japan is affected by various damaging phenomena, such as liquefaction during earthquakes (Yasuda, 2011). The Great Eastern Japan Earthquake, which occurred in 2011, lead to significant earthquake motions, tsunami, liquefaction, fire and nuclear accidents. These hazards occurred very extensively across the region. For that reason, it caused unparalleled damage and costs. The average duration of the earthquake ground motions that have occurred in the past in Japan was 60 seconds. However, during the Great Eastern Japan Earthquake, the ground motion duration was 150 seconds (Sasaki, 2012). The time period of this earthquake duration was found to lead to significant liquefaction damage. The potential for huge earthquake occurrences in Japan is a significant concern. Damage caused by this type of earthquake is assumed to be more than the Great Eastern Japan Earthquake. The influence and equivalent earthquake durations of these earthquakes are estimated to be longer due to concurrence of plural earthquakes. Similar long duration earthquakes are more likely to occur in the future. Accordingly, it is necessary for methods of suppression of liquefaction to be considered for these longer earthquake durations. Therefore, this research focuses on cement solidification, which is used as a liquefaction countermeasure and inhibition of shear deformation by additional short fibers. The apparent cohesion is thought to increase by inhibition of shear deformation. In addition, this paper reports on the results of basic research conducted on whether these techniques lead to suppression of liquefaction related to the duration of earthquakes.

2 TESTING PROCEDURE

2.1 *Purpose of this study*

This study involves the investigation of liquefaction mechanisms using a cement solidification material and tension stiffeners. The work has concentrated on gaining an understanding of the shear behavior of the cement admixture material. Furthermore, investigation of types of solidification material and different amounts of solidification material were also investigated. In addition, short fiber admixtures were included in the same investigation. The improved soils with added cement solidification and short fibers were tested using cyclic shear tests at different frequencies, to reveal the influence of duration of earthquakes.

2.2 *The materials used during this study*

Toyoura sand was used for the soil samples. Ordinary Portland cement and recycled Bassanite from waste plasterboard was used for the solidifying material. PVA fiber, with an average length of 12.0 mm was used for the tension stiffener. The fiber is a polyvinyl alcohol fiber, made by Kuraray Co., Ltd.

2.3 *Method of preparing specimens*

Specimens were prepared with a target dry density of 1.489 g/m^3, equivalent to a relative density of 60% of Toyoura sand (irrespective of the presence or absence of additional cement solidification material). Specimens were prepared using the moist tamping method. The additional additives were blended separately outside of the specimen and mixed at various percentages to the absolute dry mass of Toyoura sand. Regulation of the water content was set to 10% after mixing of

the sand, solidification material, and tension stiffener. Curing time for the specimens was 3 days.

2.4 *Test condition and method*

Table 1 shows the testing conditions. Fracture morphology of the specimens was anticipated to change due to additive percentages of solidifying material. Therefore, a target strength was set at 50 kN/m^2 for unconfined compressive strength, which is considered to be a reasonable strength against liquefaction (Zen, 1994). The additive percentage rate was set at 2% cement. In addition, recycled Bassanite only mixing gave concerns of large variation in the strength and elution of fluorine. For that reason, it was mixed with cement (C = 1% + B = 5 %). For another set of tests, the addition rate was set at 1% cement and 1% short fiber. The termination condition of the drained monotonic shear test and undrained monotonic shear test is when axial strain of 15% is reached. Undrained cyclic shear tests were carried out under sine-wave stress control with a load speed of 0.1 Hz. In addition, the degree of saturation (Skempton's B) of the specimens in all conditions was more than 0.96. The frequency of number of repetitions over the same time period was substituted for duration of the ground motions.

3 RESULTS AND DISCUSSIONS

3.1 *Suppression method of liquefaction by solidification*

Table 2 shows the strength parameters determined with Mohr's stress circles from the drained monotonic shear tests. For the case of C = 0%, cohesion is 0 kN/m^2. On the other hand, for the case of C = 2%, cohesion is increased to 27.3 kN/m^2 by the addition of cement. Additionally, for the case of C = 1%+B = 5%, cohesion is found to increase to 36.4 kN/m^2 due to the addition of recycled Bassanite. The increase of liquefaction resistance is induced by the cohesion.

Figure 1 (a) - (c) shows the effective stress path diagram for each condition resulting from the undrained cyclic shear tests. For the case of C = 0%, effective stress is decreased with

increased number of cycles and shows cyclic mobility. This shows a typical liquefaction behavior for sand. For the case of C = 2% and C = 1% + B = 5%, in the event of addition of solidification material, the number of cycles is increased irrespective of the double cyclic stress ratio. The stress path for mixing solidification material shows cyclic mobility after reaching the phase transformation lines (PT line). The reason for this behavior is a interparticles forces for the sand with solidification.

Figure 2 shows the relationships between number of cycles and maximum pore pressure ratio for each solidification material additive condition. For the case of C = 0%, the trend changes from about $\tau / p_c' = 0.6$, as it reaches liquefaction. In contrast to this, for the case of added solidification material, greater excess pore water pressure occurs in early phases of shear, because the cyclic deviator stress ratio is high. Since the maximum pore pressure ratio 1.0 is reached slowly, liquefaction is not reached as quickly. In the case of recycled Bassanite, the excess pore water pressure ratio does not reach 1.0. This is thought to suppress pore pressure development between the sand particles due to the solidification material. The excess pore pressure is suppressed by the cement solidification effect and the toughness of the recycled Bassanite.

Figure 3 shows the relationships between number of cycles and double amplitude axial strain. For the case of C = 0%, the strain increased significantly just before liquefaction. On the other hand, for the case of C = 2%, the strain increases in the early phases of shear with the development of excess pore pressure. Then, the strain progresses slowly before reaching DA = 5%. Additionally, for the case of C = 1% + B = 5%, the strain increases more slowly than for the case of C = 2%.

Table 2. Strength parameter

Additive conditions (%)	Cohesion c' (kN/m^2)	Internal friction angle ϕ' (°)
C = 0	0.0	34.0
C = 2	27.3	35.0
C = 1 + B = 5	36.4	33.0

Table 1. Test condition

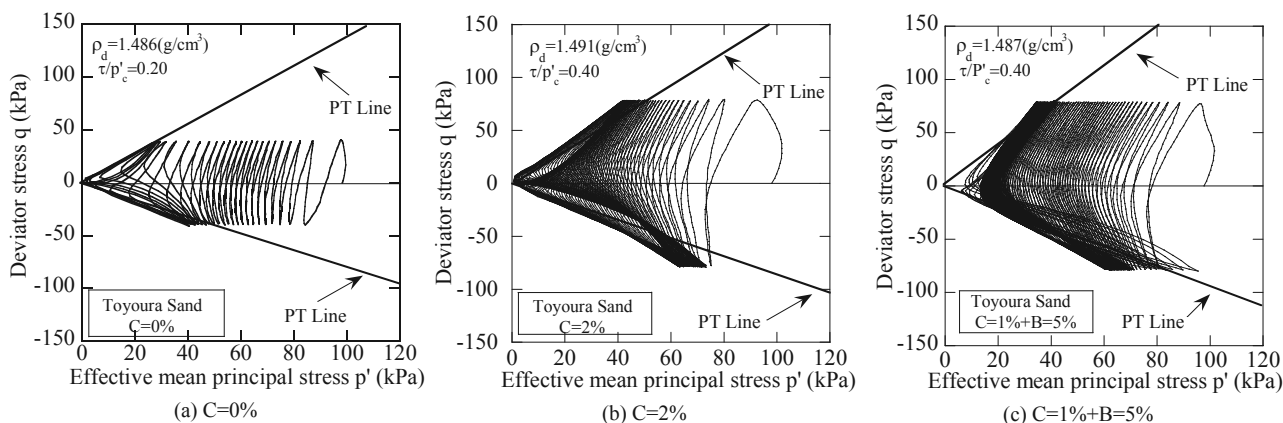| Examination item	Method of preparing specimens	Water content (%)	Additive rate(%)			Target dry density (g/cm^3)	Curing days	Confining pressure of triaxial test (kPa)
			C	B	F			
Toyoura sand	Tamping method	10	0			1.489	0	30 50 100 200
Toyoura sand +Cement (C)			2	0	0		3	
Toyoura sand +Recycled bassanite (B)			1	5	0			
Toyoura sand +PVA fiber (F)			1	0	1			

(a) C=0%   (b) C=2%   (c) C=1%+B=5%

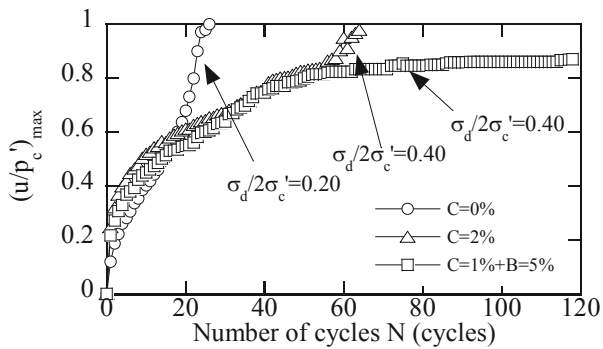Figure 1. Effective stress path diagram

Figure 2. The relationships between number of cycles and max pore pressure ratio
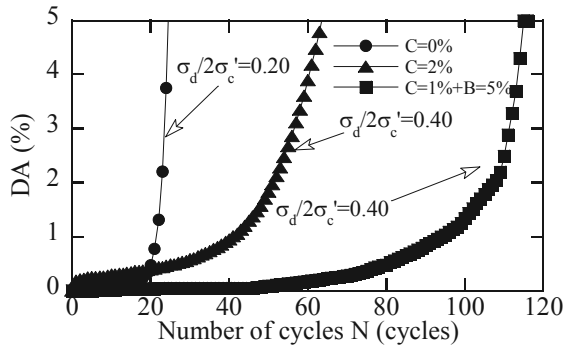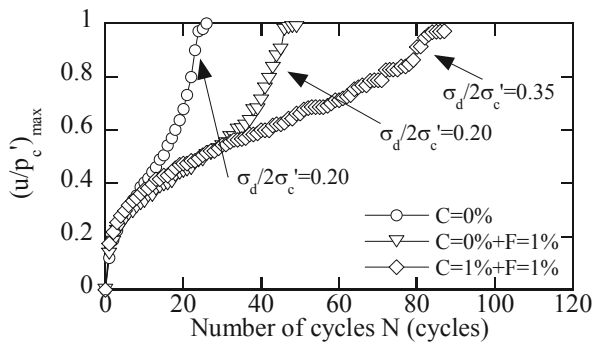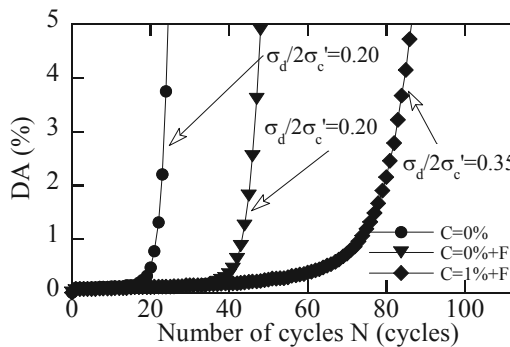

Figure 3. The relationships between number of cycles and double amplitude axial strain

Figure 4 shows the liquefaction strength curve. For this study, we assume that liquefaction occurs at DA = 5 %. Focusing on the liquefaction strength N_{20}, the improved soils increased liquefaction strength by about 2.5 times, compared to non-improved soil. The liquefaction strength required for an earthquake of M 9.0 class such as the Great East Japan Earthquake is assumed to be 34 times (Sezaki, 2011).
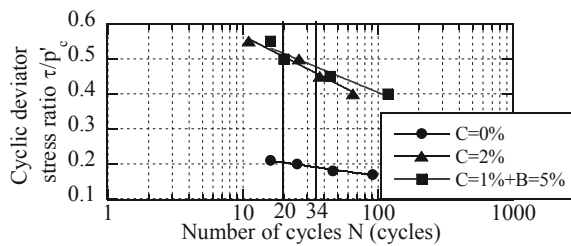
Figure 4. Liquefaction strength curve
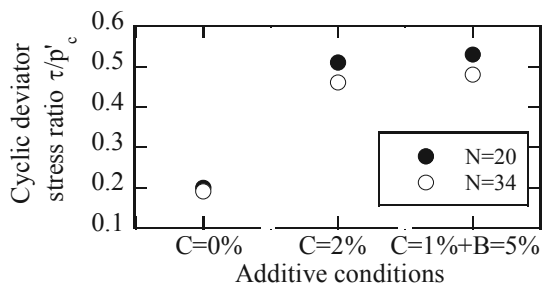
Figure 5. The relationships between additive conditions and liquefaction strength

Figure 5 shows the relationships between additive conditions and liquefaction strength. For the case of liquefaction strength N_{20}, the liquefaction strength with mixing of solidification material makes no difference. However, for the case of liquefaction strength N_{34}, liquefaction strength of mixing recycled Bassanite increases slightly. From this, for the

case of a large earthquake, the greater the development of cohesions, the more chance there will be suppression of liquefaction due to mixing of solidification material.

3.2 Suppression method of liquefaction by tension stiffener

Table 3 shows strength parameters determined from Mohr's stress circles from the drained monotonic shear tests. The cohesion increases due to an increase of the additive ratio of tension stiffener and solidification material. These are considered to be due to the added deformation restraint of the specimens by the additional fibers and the interparticles force of sand due to the cement.

Table 3. Strength parameter

Additive conditions (%)	Cohesion c' (kN/m^2)	Internal friction angle ϕ' (°)
C = 0	0.0	34.0
C = 0 + F = 1	24.2	40
C = 1 + F = 1	64.6	40.5

Figure 6 (a) - (c) shows the effective stress path diagrams for each condition for the undrained cyclic shear tests. (a) C = 0% and (b) C = 0% + F = 1% have the same cyclic stress ratio. Focusing on the stress path (b) C = 0% + F = 1%, the decrease in effective stress due to cycles is small due to the additional fibers. The number of effective stress cycles path until the PT line is however increased. It can be seen that there is an effect of increasing the liquefaction resistance even with the addition of only fibers. Then, for the case of (c) C = 1% + F = 1%, the number of cycles for liquefaction is increased, regardless of cyclic stress ratio. Cyclic mobility occurs after reaching the PT line with increasing the additive ratio of the short fibers and solidification material. These are thought to increase the liquefaction resistance by restraint of deformation of the short fibers and the interparticles forces of the sand due to the added cement.

Figure 7 shows the relationships between number of cycles and maximum pore pressure ratio for each conditions. The development of the excess pore pressure ratio of non-improved soil and for the addition of only short fibers reaches liquefaction after it reaches $\tau/p_c' = 0.6$. Next, in the case of added short fibers and solidification material, significant excess pore pressure ratio occurs in early phases of the shear, because the cyclic deviator stress ratio is great. But, the liquefaction does not rise instantly. The excess pore pressure ratio approaches $\tau/p_c' = 1.0$ at a slow pace. This is thought to reflect the restraint of deformation for cyclic behaviors depending on the addition of short fibers and solidification material.

Figure 8 shows the relationships between number of cycles and double amplitude axial strain. This figure indicates, that the additional short fibers suppress the deformation to liquefaction. Additionally, for the case of added solidification material, the deformation does not advance instantly, even though the effective stress is close to 0. The deformation reaches high values at a slow pace.

Figure 9 shows the liquefaction strength curve. The liquefaction strength for the addition of only short fibers shows a little strength increase. In contrast to this, significant strength increase is shown by adding more solidification material.

Figure 10 shows the relationships between additive conditions and liquefaction strength. Liquefaction countermeasures can be created by the addition of certain solidifying material. Interestingly it is seen that more addition of short fibers can also reduce the amount of solidification material. This method may make effective use of waste by

4. CONCLUSIONS

(1) The liquefaction resistance is increased, due to the increase of cohesion from the added solidification material. For the added solidification material, the interparticles forces of sand due to this cohesion suppresses liquefaction. The magnitude of the suppression effect of liquefaction is influenced by the interparticles forces of the sand.

(2) The effect of shear deformation suppression also increases due to the development of apparent cohesion. For the case of short fiber and solidification material, liquefaction is suppressed by the cohesion of solidification material and shear deformation suppression.

(3) It is considered from the study results that, the utilization of discharged wood waste by the earthquake will have a similar effect as the effect of shear deformation suppression

of the short fibers. Additionally, the effectiveness of the

utilization of recycled Bassanite has been verified. In the future, it is important to study the suppression technique for a variety of earthquakes, focusing attention on not only suppression of liquefaction, but also recycling costs.

5. ACKNOWLEDGEMENTS

6. REFERENCES

Yasuda S. 2011. The liquefaction damage of KANTO. Board of Tohoku-Pacific Ocean Earthquake disaster investigation report (in Japanese).

Sasaki T. 2012. River bank and liquefaction. Public Works Research Institute, http://www.pwri.go.jp/

Zen K. 1994. Remedial Measures for Reclaimed Land by Premixing Method. *The Japanese Society of Soil Mechanics and Foundation Engineering*, Vol.42, No.2, 37-42 (in Japanese).

Sezaki M. 2011. Liquefaction and slope failures in the Great East Japan Earthquake. *Text of road technology workshops* (in Japanese).

Figure 7. The relationships between number of cycles and max pore pressure ratio

Figure 9. Liquefaction strength curve

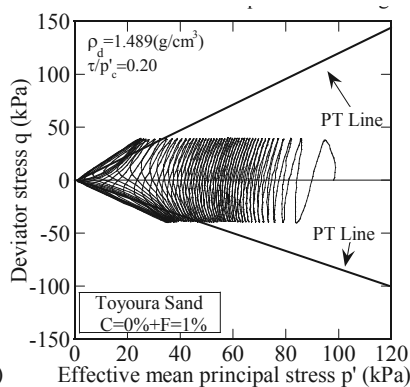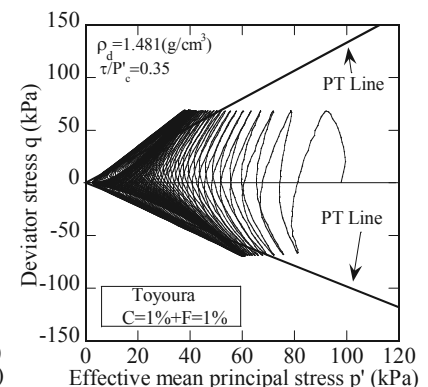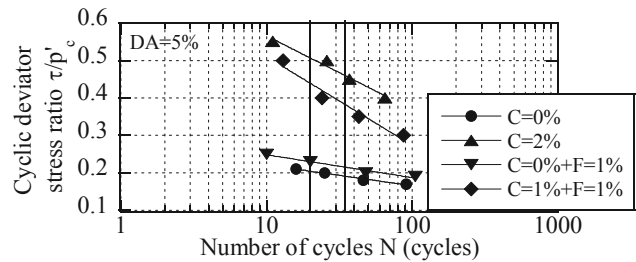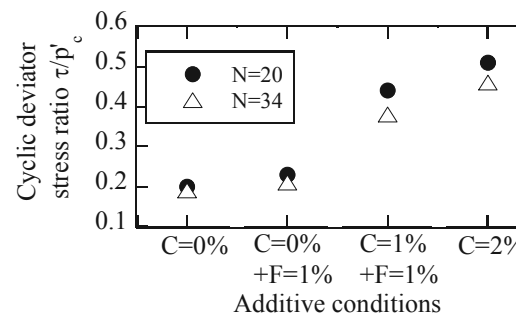Figure 8. The relationships between number of cycles and double amplitude axial strain

Figure 10. The relationships between additive conditions and liquefaction strength
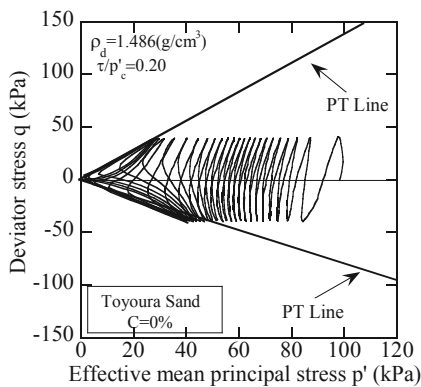
(a) C=0%

(b) C=0%+F=1%

(c) C=1%+F=1%

Figure 6. Effective stress path diagram